

Object-oriented mapping in dynamic environments

Matti Pekkanen, Francesco Verdoja and Ville Kyrki

Abstract—Grid maps, especially occupancy grid maps, are ubiquitous in many mobile robot applications. To simplify the process of learning the map, grid maps subdivide the world into a grid of cells, whose occupancies are independently estimated using only measurements in the perceptual field of the particular cell. However, the world consists of objects that span multiple cells, which means that measurements falling onto a cell provide evidence on the occupancy of other cells belonging to the same object. This correlation is not captured by current models. In this work, we present a way to generalize the update of grid maps relaxing the assumption of independence by modeling the relationship between the measurements and the occupancy of each cell as a set of latent variables, and jointly estimating those variables and the posterior of the map. Additionally, we propose a method to estimate the latent variables by clustering based on semantic labels and an extension to the Normal Distributions Transfer Occupancy Map (NDT-OM) to facilitate the proposed map update method. We perform comprehensive experiments of map creation and localization with real world data sets, and show that the proposed method creates better maps in highly dynamic environments compared to state-of-the-art methods. Finally, we demonstrate the ability of the proposed method to remove occluded objects from the map in a lifelong map update scenario.

I. INTRODUCTION

Mapping is a central functionality in any mobile robot system, as accurate maps are required for foundational mobile robot tasks such as localization and path planning. Grid maps, most ubiquitous of which is the 2D occupancy grid map, discretize the environment into a grid of cells, which are assumed to be independent of each other such that only the measurements directly evaluating a cell as occupied or free are taken into account when estimating the occupancy of that cell.

This assumption is admissible when assuming the environment is static, and while it is known that it is not entirely true, cells are assumed independent to reduce the complexity of the task of learning the map.

However, a single object often occupies more than one cell, which means that measurements from all cells occupied by the same object can be used to infer the occupancy of all object's cells. For example, if the object is partially occluded, the evidence from the visible cells should be used to infer the occupancy of the occluded cells. If the object has vacated and this is not done, the map will contain erroneously retained cells which may cause problems in localization or path planning, as shown in Figure 1.

This work was supported by Business Finland, decision 9249/31/2021. We gratefully acknowledge the support of NVIDIA Corporation with the donation of the Titan Xp GPU used for this research.

M. Pekkanen, F. Verdoja and V. Kyrki are with School of Electrical Engineering, Aalto University, Espoo, Finland. {firstname.lastname}@aalto.fi

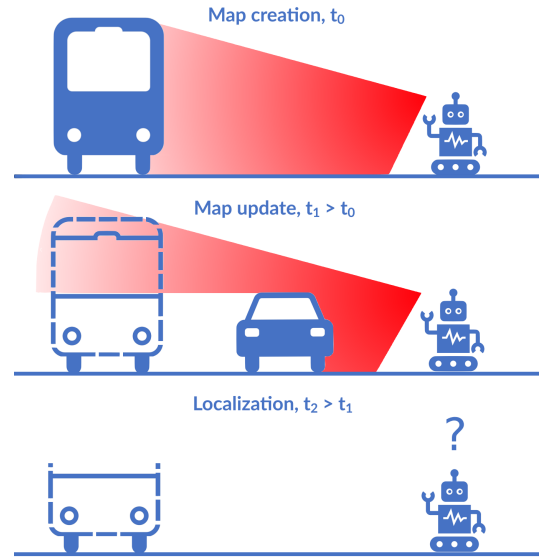


Fig. 1: Occlusion and dynamic objects constitute the main source of mapping errors. When not treated properly, partial objects and other residual noise is left on the map.

In this work we formalize the theory of grid mapping with relaxed cell-independence assumption, and propose a way to use all measurements to update the cells in a grid map by jointly estimating the posterior occupancy of the map as well as a set of latent variables which describe a correspondence between the cells occupied by the same object, representing the object-oriented nature of the environment.

The benefit of this method is that more evidence is used for occupancy estimation by aggregating the evidence from the cells occupied by the same object, making the map update faster in adjusting to the environment's dynamics. Additionally we can infer the occupancy of occluded cells belonging to a partially occluded object by using the observations of the visible part of the object. This reduces the number of residual cells left by occlusions, improving the map quality.

In a series of experiments, we show the performance of the proposed method in localization and map creation tasks, where the quality of the produced maps are evaluated using localization accuracy, and the number of erroneous residual cells, respectively. Additionally, we qualitatively demonstrate the performance in a lifelong map update scenario.

The main contributions of this paper are:

- i) We formalize the theory for occupancy update on non-independent cells by jointly estimating the set of latent variables that describe the relationship between the measurements and the cells for general grid maps, yielding

better quality maps in map creation and lifelong map update.

- ii) We propose a method to estimate the latent variables by clustering the cells based on their semantic labels.
- iii) We propose an extension to Normal Distributions Occupancy Map (NDT-OM) called Clustered Normal Distributions Transform Occupancy Map (C-NDT-OM) which uses the proposed method, and release the source code of the implementation.
- iv) Using C-NDT-OM, we demonstrate the map creation performance of the proposed methods in multiple experiments using real-world data, evaluating the created maps both in terms of localization accuracy as well as dynamic object removal capabilities.
- v) We qualitatively demonstrate the lifelong map update performance of the proposed methods with experiments using real-world data.

II. RELATED WORK

A. Object-oriented grid maps

The world consists of discrete objects and amorphous matter, commonly referred to as *things* and *stuff* [1], [2], respectively. While most *stuff*, especially on land, is properly represented by a grid of independent cells, many *things*, *i.e.*, objects, on other hand are not. As in [3], maps that attempt to record the latter are commonly referred to in literature as *object-oriented maps*.

The two main methods of building object-oriented grid maps are to map the dynamics caused by objects, or combining object tracking and detection systems to mapping methods. A related example of the former approach is [4], where the dynamic occupancy grid framework, proposed in [5], was extended to include object clustering based on their dynamic properties to produce 2.5D classified occupancy grid. However, unlike our work, the cells are assumed to be independent and only measurements directly measuring the cell occupied or free are used for the cell state estimation, whereas we use the whole set of measurements to estimate the cell occupancy.

The combination of object detection and tracking and Simultaneous Localization and Mapping (SLAM) on occupancy grid was proposed in [6] and further extended in [7] to track and update moving and movable objects. Unlike our work, the objects are stored in separate maps, and the cells are assumed to be independent within the object. In [8] the tracked dynamic objects are removed and added on the map after each step removing the object trails. However, the cells are assumed to be independent, and the static and dynamic parts of the environment cannot overlap. Unlike that work, we can model the extent of the object and represent movable objects that can be updated in lifelong scenario.

B. Updating grid maps

Map update means adding evidence to the map. If the world would be static, there would be no contradictory information besides noise. However, in the real world maps must be able to adjust to changing environment states.

Occupancy grids [9] adjust to changing environments slowly, as all of the evidence gathered is taken into account. A solution to this problem is to consider only a fixed number of the latest measurements, enabling the map to adjust to environment dynamics [10], [11], or filtering the dynamic objects from the measurements [12].

For the same reason as to why object detection and tracking methods mainly do not use grid maps, most research in the field of object-oriented visual slam [3], [13] and semantic mapping [14]–[17] use continuous map representations. While these methods can represent objects' extent naturally, the probabilistic formulation of the occupancy of continuous space is still unsolved. On the other hand the grid maps can model the occupancy of the space probabilistically, and in this work we propose a method to include objects' extent into a grid map.

Lifelong localization and mapping refers to the problem of keeping the map of the environment up-to-date while the robot operates. While there are many ways to achieve this, graph sparsification methods update the map. However, the majority of methods assume a static environment, and those that do not rely on replacing the measurements with newer ones [18] or by naively combining the evidence [19]. In [20] a fusion method is presented, but it does not estimate the occupancy or probability of the update. Unlike the aforementioned methods, our work explicitly fuses the acquired evidence with the ability to remove vacated objects and to add new objects.

C. Normal Distributions Transform (NDT)

Dimensionality is one of the main problems with grid mapping. To alleviate this problem NDT [21] represents the contents of a cell as a normal distribution, a sub-cell resolution representation which allows the cell size to grow.

To use NDT maps in dynamic environments, the occupancy update with a fixed window of measurements was incorporated into the map, yielding NDT-OM [22]. Another approach was presented in [19], where dynamic objects were detected comparing subsequent measurements and clustered. By estimating the cluster dynamics, the occupancy of the objects were propagated in the map, decaying unobserved dynamic objects.

Semantic NDT maps [23] enable better understanding of the environment content and dynamics. However, in [23], separated submaps are built for each label; in contrast, in our work we store the entire distribution of the measured labels, allowing more detailed use of the voxel labels. Additionally, all of the presented methods retain the independent cells and measurements, whereas our method leverages the complete set of measurements to update the map.

III. PROBLEM STATEMENT

The generic occupancy mapping problem is defined as finding a point estimate for the distribution $p(m_t | z_{0:t}, x_{0:t})$, where $m_t = \{m_t^0, \dots, m_t^n\}$ is the map at time t and m_t^i are the individual cells of the map, $x_{0:t} = \{x_0, \dots, x_t\}$ is the sequence of states, *i.e.*, the estimated poses, and

$z_{0:t} = \{z_0, \dots, z_t\}$ the sequence of measurements. Under the assumption that the cells are independent from each other, the map distribution can be solved by estimating the state of each cell individually. Additionally it is generally assumed implicitly that only the measurements on whose perceptual field the cell is in—hereafter referred to as measurements *falling onto* the cell—are used to update the cell. This yields the general formulation of the mapping problem as $\max_m p(m_t | z_{0:t}, x_{0:t}) = \max_m \prod_i p(m_t^i | z_{0:t}^i, x_{0:t})$, where $z_{0:t}^i$ is the set of measurements falling onto the cell m^i . This is depicted in Figure 2a.

However, since the world consists of objects that span multiple cells, measurements falling onto multiple cells represent parts of the same object, and therefore affect the occupancy of a single cell. This means that there exists a set of dependencies between the cells and measurements, and knowing these dependencies allows us to take into account all measurements when estimating the occupancy of a single cell.

Let $d_t^{(i,j)}$ be a latent variable that models the effect on the cell m^i of the measurements z^j , *i.e.*, those falling onto the cell m^j , at time t ; also, let \mathcal{D}_t be set of latent variables d_t between all pairs of cells in the map. Using these definitions we can improve our estimate of the occupancy of a cell m^i by augmenting the measurement model by taking into account the whole set of measurements $p(m_t^i | \mathcal{D}_t, z_{0:t}, x_{0:t}) = p(m_t^i | z_{0:t}^i, d_t^{(i,i)}, \dots, z_{0:t}^j, d_t^{(i,j)}, x_{0:t})$ which, given the latent variables \mathcal{D}_t , are independent from each other

$$p(m_t^i | \mathcal{D}_t, z_{0:t}, x_{0:t}) = \prod_j p(m_t^i | z_{0:t}^j, d_t^{(i,j)}, x_{0:t}) , \quad (1)$$

which is depicted in Figure 2b.

To be able to use the augmented sensor model, we start by jointly estimating the occupancies and the latent variables

$$p(m_t, \mathcal{D}_t | z_{0:t}, x_{0:t}) = p(m_t | \mathcal{D}_t, z_{0:t}, x_{0:t}) \cdot p(\mathcal{D}_t | z_{0:t}, x_{0:t}) , \quad (2)$$

and given that the latent variables \mathcal{D}_t fully characterize the dependencies between each cell in the map, the cells of the map are conditionally independent of each other given \mathcal{D}_t , therefore we can solve each cell independently

$$p(m_t, \mathcal{D}_t | z_{0:t}, x_{0:t}) = \prod_i p(m_t^i | \mathcal{D}_t, z_{0:t}, x_{0:t}) \cdot p(\mathcal{D}_t | z_{0:t}, x_{0:t}) . \quad (3)$$

By marginalizing over the latent variables we acquire the posterior distribution of the map occupancy. The problem is to find a point estimate to

$$\max_m p(m_t | z_{0:t}, x_{0:t}) = \max_m \int p(m_t | \mathcal{D}_t, z_{0:t}, x_{0:t}) \cdot p(\mathcal{D}_t | z_{0:t}, x_{0:t}) \mathcal{D}_t . \quad (4)$$

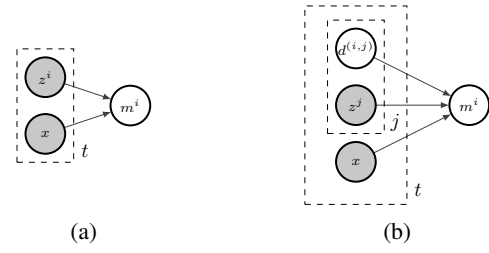


Fig. 2: Inverse sensor model of the generic mapping method (a) and the proposed method (b). The vertices in gray, are assumed to be known, while the vertices in white, *i.e.*, the map cells m^i and the latent variables $d^{(i,j)}$, are unknown. We present the inverse sensor model instead of the usual likelihood model for clarity.

IV. METHODS

Marginalizing over the latent variables \mathcal{D}_t is intractable, therefore we simplify the expression by assuming that the point estimate for the posterior is acquired by

$$\max_m \int p(m_t | \mathcal{D}_t, z_{0:t}, x_{0:t}) \cdot p(\mathcal{D}_t | z_{0:t}, x_{0:t}) \mathcal{D}_t \simeq \max_m p(m_t | \mathcal{D}_t, z_{0:t}, x_{0:t}) \cdot \max_{\mathcal{D}} p(\mathcal{D}_t | z_{0:t}, x_{0:t}) . \quad (5)$$

This splits the estimation problem into two parts. In Section IV-A we propose a way to estimate $\max_m p(m_t | \mathcal{D}_t, z_{0:t}, x_{0:t})$, and in Section IV-B we propose a way to estimate $\max_{\mathcal{D}} p(\mathcal{D}_t | z_{0:t}, x_{0:t})$.

A. Measurement model

The measurement model $p(m_t^i | \mathcal{D}_t, z_{0:t}, x_{0:t})$ is an extension to the standard inverse sensor model $p(m_t^i | z_t^i, x_t)$ such that it takes into account the evidence gained from the other cells in the map, weighted by the latent variables \mathcal{D}_t , as show in (1). The extended update term is implemented in log odds form as

$$l(m_t^i) = \sum_j \log \frac{p(m_t^i | z_t^j, x_t)}{1 - p(m_t^i | z_t^j, x_t)} \cdot d_t^{(i,j)}$$

$$l(m_{0:t}^i) = l(m_{0:t-1}^i) + l(m_t^i)$$

$$\max_m p(m_t^i | \mathcal{D}_t, z_{0:t}, x_{0:t}) = 1 - \frac{1}{1 + \exp\{l(m_{0:t}^i)\}} , \quad (6)$$

which implements a binary Bayes filter yielding the maximum a posteriori estimate of the cell occupancy probability. It is noteworthy that when $\mathcal{D}_t = \{\forall m_t^i m_t^j \in m_t : j \neq i, d_t^{(i,j)} = 0\} \cup \{\forall m_t^i \in m_t : d_t^{(i,i)} = 1\}$, the problem resolves back to the original mapping problem with independent cells.

B. Estimation of the latent variables

The intuition behind the latent variables \mathcal{D}_t is that the environment consists of objects that span multiple cells, and a positive latent variable between two cells reflects the fact that the same object is occupying both cells. This makes the relationship symmetric, and therefore we model the environment as *clusters* $c \subseteq m$ representing the objects in the environment. All the elements in a cluster are cells that are dependent on each other, *i.e.*, $\forall m^i m^j \in c, d^{(i,j)} > 0$.

In a map with n cells, there are n^2 latent variables in \mathcal{D}_t . Therefore instead of estimating the pairwise latent variables between each two cells in the map, we estimate the *membership* δ^i of the cell m^i to a cluster c . We assume that clusters form a partition of the cells of the map, therefore the number of clusters $n_c \leq n$. From this, the entire set of latent variables \mathcal{D}_t is recoverable by choosing $\{\forall m^j \in c : d^{(j,i)} = \delta^i\}$ for all clusters.

While any clustering approach can be employed to estimate \mathcal{D}_t , in this work we implement it as a region growing algorithm [24] based on the cell semantics. Each voxel is initialized as a seed cluster; then, after each measurement, region growing steps are performed, where all neighboring clusters are compared using a similarity metric

$$s = \begin{cases} 1, & l_a = l_b \\ 0, & \text{otherwise} \end{cases}, \quad (7)$$

where l_a and l_b are the majority semantic labels of the clusters a and b , respectively, as estimated through semantic segmentation. If $s = 1$, the cluster are joined, otherwise they are not. This step is iterated until no more clusters can be joined or a maximum iteration limit is reached. A similarity metric based on the Kullback-Leibler divergence between the label distributions was tested, but the simpler metric proved to be sufficiently accurate while computationally lighter.

The membership is estimated using the Pearson's χ^2 test, which determines whether two categorical distributions are independent of each other.

In an occupancy grid map, each measurement is either providing evidence for the cell being occupied or empty. Therefore the measurements form a categorical distribution with two categories *occupied* and *empty*, and the estimates of each category for a cell m^i are denoted as o^i and e^i , respectively. The same quantities over the whole cluster c can be calculated as well, but the evidence is weighed according to the membership of that cell to the cluster. Therefore the evidence of *occupied* over the cluster c is

$$o^c = \sum_{m^j \in c} \delta^j \cdot o^j, \quad (8)$$

and the evidence of *empty* e^c is computed similarly. This allows us to estimate the membership δ^i of the cell m^i in the cluster c

$$\delta^i = \chi^2 \left(\frac{(o^i - o^c)^2}{o^c} + \frac{(e^i - e^c)^2}{e^c} \right). \quad (9)$$

If the evidence of the cell and the cluster align very well, it is likely that the cell is a member of the cluster. However, if the evidence differ significantly, it is likely that the cell is no longer a member of the cluster. This may happen for various reasons, such as the original cluster having moved away, and a new object occupying the cell.

The NDT-OM measurement model $p(m_t^i | z_t, x_t)$ is used in this work, which is described in detail in [22]. Instead of directly counting the rays that pass through the voxel as empty observations, in NDT-OM the probability $p(x_{ML} | z_i)$ is estimated whether the ray passed through the distribution

TABLE I: Oxford Radar RobotCar sequences used in the localization experiment.

Name	Date	Time
sequence 1	1/10/2019	11:46:21
sequence 2	1/10/2019	12:32:52
sequence 3	1/11/2019	12:26:55
sequence 4	1/14/2019	12:05:52
sequence 5	1/15/2019	13:06:37
sequence 6	1/16/2019	13:09:37
sequence 7	1/17/2019	11:46:31
sequence 8	1/18/2019	12:42:34

or not. A threshold $p_{th} = 0.5$ is set for the probability whether the measurement is counted as *occupied* or *empty*. Additionally NDT-OM contains a scaling factor $\eta \in [0, 0.5]$ that control the adaptation rate of the map. Following common practice, $\eta = 0.2$ is used unless otherwise stated.

C. C-NDT-OM

In this work we propose an extension to NDT-OM [22], the C-NDT-OM. NDT-OM divides the environment into a regular 3D grid of cells, with each cell m^i represented by a 3D normal distribution $\mathcal{N}(\mu^i, \Sigma^i)$, number of measurements N^i and the probability of the cell being occupied $p(m^i | z_{0:t})$.

In C-NDT-OM, the cell definition is extended by storing the cluster index c , cluster membership δ^i , and the categorical distribution of semantic labels $p(l | \vec{p})$, yielding the augmented cell definition of $m^i = \{\mu^i, \Sigma^i, N^i, p(m^i | z_{0:t}), p(l | \vec{p}), c, \delta^i\}$. This gives us the definition of the C-NDT-OM as a set of cells $m_{cndt} = \{m^i, \dots, m^n\}$.

V. EXPERIMENTS

The three main questions we want to answer with the experiments are:

- 1) Does the localization accuracy improve using the proposed object-oriented map update method?
- 2) Does the number of residual cells caused by dynamic objects reduce when using the proposed object-oriented map update method?
- 3) Does the number of residual cells caused by movable objects reduce in a lifelong localization scenario using the proposed object-oriented map update method?

To answer these questions we compared the proposed mapping method to the state-of-the-art baseline method, NDT-OM, in a series of experiments¹.

In the first experiment (Section V-A) we created a map with each method, and performed seven localization experiments on each of the maps, and evaluated the localization accuracy. In the second experiment (Section V-B), we created 11 maps with each method and counted all the dynamic cells in the map as a metric of how well the methods can cope with dynamic objects. Finally, we demonstrated the capabilities of the proposed mapping method on lifelong update scenario (Section V-C).

¹The source code of the implementation will be made publicly available upon the acceptance of this work.

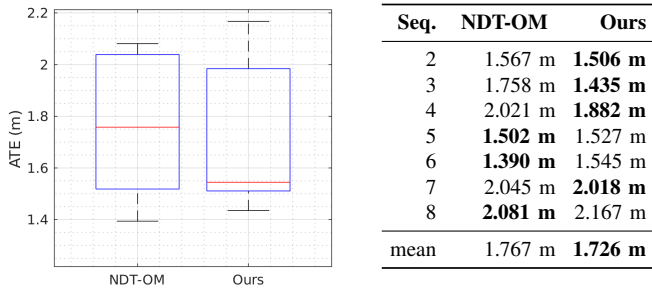


Fig. 3: The results of the localization experiment in terms of Absolute Trajectory Error (ATE). The red line is the sample median, the black dashed line presents the sample interval and the blue box ranges from its first to third quartile.

A. Localization experiment

The Oxford Radar RobotCar data set [25], [26] was used in the localization experiment which consists of multiple traversals through the same route. Eight sequences were chosen from the data set, presented in Table I, containing in total over 265k laser scans. Sequence 1 was chosen for map building, and sequences 2-8 for localization. The first sequence from each day of the data set was chosen, except for sequences 5 and 6, where the first sequences suffered from prolonged losses of Global Navigation Satellite System (GNSS) fix, making the ground truth unreliable. The data set contains data from two Velodyne 32E lasers, and only the measurements from the left laser were used, as they were sufficient for the experiment. The semantic segmentation of the laser point clouds was obtained using RandLA-net [27], with a pre-trained model provided by the authors.

For both the baseline NDT-OM and the proposed mapping method, we employed NDT-OM’s fusion method [28] using ground truth poses provided by the data set. Voxel size of 0.6 m and submaps with (x, y, z) -dimensions of $(200, 200, 20)$ m were used.

Normal Distributions Transform Monte-Carlo Localization (NDT-MCL) [29] was used as a localization method in the experiment using the same motion model as in the original paper. The Inertial Navigation System (INS) was used as odometry. Localization was initialized around the known initial pose x_0 with uniform distribution with dimensions $[-20, 20]$ m on xy -axes and $[0, 2\pi]$ rad in ψ . All of the experiments were run at $0.2\times$ real time. All parameters were chosen using practical experience with the methods. The estimated pose was stored at each time step, as well as the ground truth, which were compared in terms of ATE [30].

The implementations of NDT-OM fusion and the NDT-MCL were based on [31]–[34].

B. Mapping experiment

The Semantic Kitti data set [35], [36] was used in the mapping experiment as the data set provides ground truth semantic labels. The data set contains measurements from a Velodyne HDL-64E laser, and given ground truth poses which were used for map building. Maps were created with

TABLE II: The results of the mapping experiment over the Kitti sequences in terms of the density of dynamic voxels in each map. These results can be divided into two groups based on the environment dynamics (fourth column).

Sequence	NDT-OM	Our method	Dynamics
04	4.582	2.893	high
01	3.426	2.298	high
mean	4.004	2.595	
07	0.508	0.831	low
10	0.308	0.539	low
09	0.478	0.325	low
08	0.301	0.344	low
05	0.182	0.185	low
03	0.176	0.138	low
02	0.078	0.103	low
00	0.073	0.094	low
06	0.037	0.073	low
mean	0.238	0.293	

each method as presented in Section V-A from all of the sequences of the data set where ground truth poses were provided, *i.e.*, sequences 00-10. Thus, in total, 11 maps were created per method.

After the maps were created, the number of dynamic cells, *i.e.*, cells with a dynamic majority label, *i.e.*, labels 252-259, were counted. This measures how well the map update can remove dynamic objects from the maps. Ideally, there would be a small number of dynamic cells, as the dynamic objects constitute a very small portion of the map. But as the dynamic objects move, the cells previously occupied by the object remain occupied and have to be emptied. Therefore a lower number of dynamic cells indicates increased ability to remove the trails left by the dynamic objects in the map. As the sequences are of different length, the number of dynamic cells is normalized by the length of the sequence, providing the final measure: the density of dynamic cells.

C. Lifelong map update experiment

In the lifelong update experiment, the Oxford Radar RobotCar data set was used. This data set was selected as it consists of multiple traversals along the same route, allowing objects to have moved between sequences, therefore requiring lifelong map update. The sensor setup, semantic segmentation, map creation and localization methods are the same as presented in Section V-A.

Sequence 1 was chosen for map building, and a sequences 2 and 6 were chosen for localization. This allows to evaluate the lifelong map update quality of the methods. We compared the methods with the nominal value of $\eta = 0.2$, as well with the maximum adaptation rate $\eta = 0.5$.

As there are no readily available metrics to evaluate the quality of the map, we present a qualitative demonstration of the capabilities of our method compared to the baseline.

D. Results

1) *Localization experiment*: The results of the localization experiment, presented in Figure 3, can be divided into two

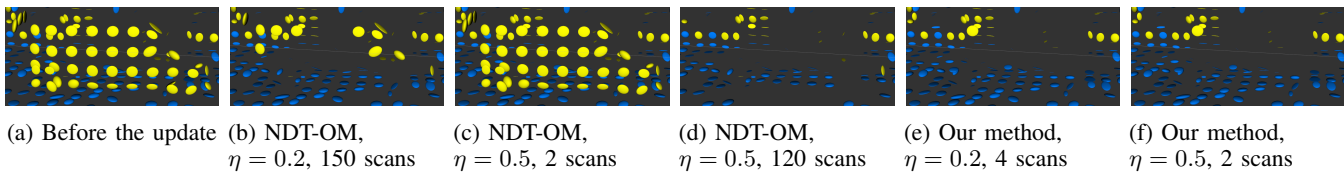


Fig. 4: The initial map (a) is updated in lifelong scenario with NDT-OM (b) - (d), and our method (e) and (f). Our method outperforms NDT-OM in update speed.

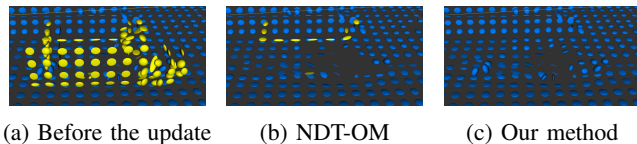


Fig. 5: The initial map (a) is updated in lifelong scenario with NDT-OM (b) while our method (c) removes the occluded parts of the object.

categories. In environments where NDT-OM performs well, our method does not yield benefits, but rather introduces errors due most likely to the noisy semantic labels. We expect that in presence of higher quality labels, the performance of our method would increase.

However, when the environment is more dynamic and the error in NDT-OM starts to grow, our method starts to yield advantages over NDT-OM, providing the lower overall sum, median, and mean ATE over all of the sequences. While the differences are small, they point towards the conclusion that our method is able to address some of the failure modes of NDT-OM in dynamic environments.

2) *Mapping experiment*: The results of the mapping experiment, presented in Table II, can be divided into two categories based on sequences with high and low dynamics. Sequences 01 and 04 of the data set contains considerably more dynamic objects than the other data sets, which can be clearly seen from the dynamic densities. In highly dynamic environments our method clearly outperforms NDT-OM, resulting in fewer residual cells from dynamic objects. In cases with few dynamic objects NDT-OM performs on average slightly better, but the differences are minor and not consistent over all sequences. The results support the proposition that our method functions well in generic environments, and especially well in highly dynamic environments.

3) *Lifelong map update experiment*: From the qualitative results of the lifelong experiment presented in Figures 4 and 5 we can see that our method is capable of delivering the intended benefit: when parts of the object are occluded, the cluster-based update is able to correctly remove the occluded parts of the object along with the observed removal of the cells (Figure 5c). Another key difference is speed (Figure 4): our method can remove the vehicle after only 4 scans, whereas even after all scans measuring of that vehicles before moving away (*i.e.*, 150 updates), with NDT-OM, parts of the vehicle is still in the map.

Moreover, the effect of adaptation parameter η is demonstrated in Figure 4. When using the maximum adaptation rate of $\eta = 0.5$, the NDT-OM eventually removes the

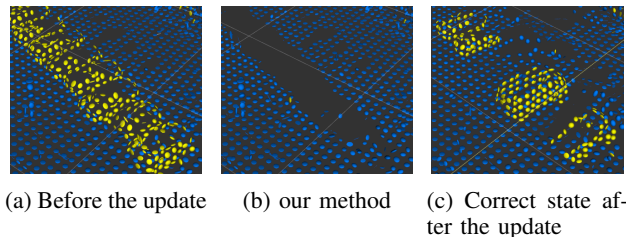


Fig. 6: The initial map (a) is updated in lifelong scenario with our method (b). The correct state after the update is shown in (c). Our method erroneously clusters all of the vehicles into a single cluster and removes the whole cluster.

vehicle after 120 scans, our method clearly outperforms NDT-OM after only 2 scans. Our method can remove the vehicle consistently with fewer scans and with lower values of η . This demonstrates that our method improves upon the capabilities of NDT-OM.

The most common failure mode of our method is the erroneous joining of disjoint clusters of the same label due to their proximity. However, in environments with sufficient static structure, the false removal of semi-static structures is considered to be less problematic than false matching of the objects. This phenomena can be clearly seen in a tightly occupied parking lot presented in Figure 6 where all cars are clustered and removed together. A more advanced clustering method would limit this behavior.

VI. CONCLUSION

In this work we formalized a relaxation of the independence of cells in grid maps by modeling the dependence of cells being occupied by the same object. This allows for more evidence to be used to estimate the cell occupancies, making the update faster and allowing the inference of the occupancy of the occluded parts of the map.

The localization accuracy and the dynamic object removal capabilities of the proposed methods were shown to improve both in map creation and lifelong update. We expect the benefits of the proposed method to go beyond localization: the residual cells left by vacated objects can be problematic in path planning; if a path is blocked, a suitable solution might be discarded needlessly.

Moreover, one interesting implication of this study is that integrating geometric, semantic, and dynamic priors can improve occupancy mapping in dynamic environments. This suggests promising new research avenues in mapping, localization, and path planning with richer environment understanding.

REFERENCES

- [1] E. H. Adelson, "On seeing stuff: the perception of materials by humans and machines," in *Human vision and electronic imaging VI*, vol. 4299. SPIE, 2001, pp. 1–12.
- [2] A. Kirillov, K. He, R. Girshick, C. Rother, and P. Dollár, "Panoptic segmentation," in *Proceedings of the IEEE/CVF conference on computer vision and pattern recognition (CVPR)*, 2019, pp. 9404–9413.
- [3] R. F. Salas-Moreno, R. A. Newcombe, H. Strasdat, P. H. Kelly, and A. J. Davison, "Slam++: Simultaneous localisation and mapping at the level of objects," in *Proceedings of the IEEE conference on computer vision and pattern recognition (CVPR)*, 2013, pp. 1352–1359.
- [4] V. Jiménez, J. Godoy, A. Artuñedo, and J. Villagra, "Object-level Semantic and Velocity Feedback for Dynamic Occupancy Grids," *IEEE Transactions on Intelligent Vehicles (T-IV)*, pp. 1–18, 2023.
- [5] D. Nuss, S. Reuter, M. Thom, T. Yuan, G. Krehl, M. Maile, A. Gern, and K. Dietmayer, "A random finite set approach for dynamic occupancy grid maps with real-time application," *The International Journal of Robotics Research (IJRR)*, vol. 37, no. 8, pp. 841–866, 2018.
- [6] C.-C. Wang, C. Thorpe, S. Thrun, M. Hebert, and H. Durrant-Whyte, "Simultaneous localization, mapping and moving object tracking," *The International Journal of Robotics Research (IJRR)*, vol. 26, no. 9, pp. 889–916, 2007.
- [7] G. Gallagher, S. S. Srinivasa, J. A. Bagnell, and D. Ferguson, "GATMO: A Generalized Approach to Tracking Movable Objects," in *2009 IEEE International Conference on Robotics and Automation (ICRA)*. Kobe: IEEE, May 2009, pp. 2043–2048.
- [8] Y. Wang, B. Wang, X. Wang, Y. Tan, J. Qi, and J. Gong, "A fusion of dynamic occupancy grid mapping and multi-object tracking based on lidar and camera sensors," in *2020 3rd International Conference on Unmanned Systems (ICUS)*. IEEE, 2020, pp. 107–112.
- [9] A. Elfes, "Sonar-based real-world mapping and navigation," *IEEE Journal on Robotics and Automation*, vol. 3, no. 3, pp. 249–265, June 1987.
- [10] D. Arbuckle, A. Howard, and M. Mataric, "Temporal occupancy grids: a method for classifying the spatio-temporal properties of the environment," in *IEEE/RSJ International Conference on Intelligent Robots and System (IROS)*, vol. 1. Lausanne, Switzerland: IEEE, 2002, pp. 409–414.
- [11] P. Biber and T. Duckett, "Dynamic Maps for Long-Term Operation of Mobile Service Robots," in *Robotics: Science and Systems (RSS) I*. Robotics: Science and Systems Foundation, June 2005.
- [12] D. Hahnel, D. Schulz, and W. Burgard, "Map building with mobile robots in populated environments," in *IEEE/RSJ International Conference on Intelligent Robots and System (IROS)*, vol. 1. Lausanne, Switzerland: IEEE, 2002, pp. 496–501.
- [13] J. McCormac, R. Clark, M. Bloesch, A. Davison, and S. Leutenegger, "Fusion++: Volumetric object-level slam," in *2018 international conference on 3D vision (3DV)*. IEEE, 2018, pp. 32–41.
- [14] R. Ambrus, N. Bore, J. Folkesson, and P. Jensfelt, "Meta-rooms: Building and maintaining long term spatial models in a dynamic world," in *2014 IEEE/RSJ International Conference on Intelligent Robots and Systems (IROS)*. Chicago, IL, USA: IEEE, Sept. 2014, pp. 1854–1861.
- [15] M. Grinvald, F. Furrer, T. Novkovic, J. J. Chung, C. Cadena, R. Siegwart, and J. Nieto, "Volumetric instance-aware semantic mapping and 3d object discovery," *IEEE Robotics and Automation Letters (RA-L)*, vol. 4, no. 3, pp. 3037–3044, 2019.
- [16] G. Narita, T. Seno, T. Ishikawa, and Y. Kaji, "Panopticfusion: Online volumetric semantic mapping at the level of stuff and things," in *2019 IEEE/RSJ International Conference on Intelligent Robots and Systems (IROS)*. IEEE, 2019, pp. 4205–4212.
- [17] N. Dengler, T. Zaenker, F. Verdoja, and M. Bennewitz, "Online object-oriented semantic mapping and map updating," in *2021 European Conference on Mobile Robots (ECMR)*. IEEE, 2021, pp. 1–7.
- [18] A. Walcott-Bryant, M. Kaess, H. Johannsson, and J. J. Leonard, "Dynamic pose graph SLAM: Long-term mapping in low dynamic environments," in *2012 IEEE/RSJ International Conference on Intelligent Robots and Systems (IROS)*. Vilamoura-Algarve, Portugal: IEEE, Oct. 2012, pp. 1871–1878.
- [19] E. Einhorn and H.-M. Gross, "Generic NDT mapping in dynamic environments and its application for lifelong SLAM," *Robotics and Autonomous Systems*, vol. 69, pp. 28–39, July 2015.
- [20] M. T. Lázaro, R. Capobianco, and G. Grisetti, "Efficient long-term mapping in dynamic environments," in *2018 IEEE/RSJ International Conference on Intelligent Robots and Systems (IROS)*. IEEE, 2018, pp. 153–160.
- [21] P. Biber and W. Strasser, "The normal distributions transform: a new approach to laser scan matching," in *Proceedings 2003 IEEE/RSJ International Conference on Intelligent Robots and Systems (IROS) (Cat. No.03CH37453)*, vol. 3. Las Vegas, Nevada, USA: IEEE, 2003, pp. 2743–2748.
- [22] J. P. Saarinen, H. Andreasson, T. Stoyanov, and A. J. Lilienthal, "3D normal distributions transform occupancy maps: An efficient representation for mapping in dynamic environments," *The International Journal of Robotics Research (IJRR)*, vol. 32, no. 14, pp. 1627–1644, Dec. 2013.
- [23] A. Zaganidis, A. Zernitov, T. Duckett, and G. Cielniak, "Semantically Assisted Loop Closure in SLAM Using NDT Histograms," in *2019 IEEE/RSJ International Conference on Intelligent Robots and Systems (IROS)*. Macau, China: IEEE, Nov. 2019, pp. 4562–4568.
- [24] R. Adams and L. Bischof, "Seeded region growing," *IEEE Transactions on pattern analysis and machine intelligence (TPAMI)*, vol. 16, no. 6, pp. 641–647, 1994.
- [25] W. Maddern, G. Pascoe, C. Linegar, and P. Newman, "1 Year, 1000km: The Oxford RobotCar Dataset," *The International Journal of Robotics Research (IJRR)*, vol. 36, no. 1, pp. 3–15, 2017.
- [26] D. Barnes, M. Gadd, P. Murcutt, P. Newman, and I. Posner, "The oxford radar robotcar dataset: A radar extension to the oxford robotcar dataset," in *Proceedings of the IEEE International Conference on Robotics and Automation (ICRA)*, Paris, 2020.
- [27] Q. Hu, B. Yang, L. Xie, S. Rosa, Y. Guo, Z. Wang, N. Trigoni, and A. Markham, "Randla-net: Efficient semantic segmentation of large-scale point clouds," *Proceedings of the IEEE Conference on Computer Vision and Pattern Recognition (CVPR)*, 2020.
- [28] T. Stoyanov, J. Saarinen, H. Andreasson, and A. J. Lilienthal, "Normal Distributions Transform Occupancy Map fusion: Simultaneous mapping and tracking in large scale dynamic environments," in *2013 IEEE/RSJ International Conference on Intelligent Robots and Systems (IROS)*. Tokyo: IEEE, Nov. 2013, pp. 4702–4708.
- [29] J. Saarinen, H. Andreasson, T. Stoyanov, and A. J. Lilienthal, "Normal distributions transform Monte-Carlo localization (NDT-MCL)," in *2013 IEEE/RSJ International Conference on Intelligent Robots and Systems (IROS)*. Tokyo: IEEE, Nov. 2013, pp. 382–389.
- [30] J. Sturm, N. Engelhard, F. Endres, W. Burgard, and D. Cremers, "A benchmark for the evaluation of RGB-D SLAM systems," in *2012 IEEE/RSJ International Conference on Intelligent Robots and Systems (IROS)*. Vilamoura-Algarve, Portugal: IEEE, Oct. 2012, pp. 573–580.
- [31] Daniel Adolffsson, Henrik Andreasson. Graph map. [Online]. Available: https://gitsvn-nt.oru.se/software/graph_map_public.git
- [32] Daniel Adolffsson. Velodyne pointcloud oru. [Online]. Available: <https://github.com/dan11003/velodyne.pointcloud.oru.git>
- [33] Henrik Andreasson, Todor Stoyanov, Daniel Canelhas, Martin Magnusson, Jari Saarinen, Tomasz Kucner, Malcolm Mielle, Chittaranjan Swaminathan, Daniel Adolffsson. Ndt core. [Online]. Available: https://gitsvn-nt.oru.se/software/ndt_core_public.git
- [34] ———. Ndt tools. [Online]. Available: https://gitsvn-nt.oru.se/software/ndt_tools_public.git
- [35] J. Behley, M. Garbade, A. Milioto, J. Quenzel, S. Behnke, C. Stachniss, and J. Gall, "SemanticKITTI: A Dataset for Semantic Scene Understanding of LiDAR Sequences," in *Proc. of the IEEE/CVF International Conf. on Computer Vision (ICCV)*, 2019.
- [36] A. Geiger, P. Lenz, C. Stiller, and R. Urtasun, "Vision meets robotics: The kitti dataset," *International Journal of Robotics Research (IJRR)*, 2013.